HEAT INPUT EFFECT OF THE FCAW PROCESS ON THE MICROSTRUCTURE AND MECHANICAL PROPERTIES OF STRUCTURAL STEEL JOINTS

Uğur GÜROL * ⓘ

Abstract: Flux-cored wires are commonly used in structural and pipeline welding, shipbuilding, offshore constructions, and petrochemical and power generation industries. The higher heat inputs in the multi-pass welding result in shorter production time while considerably changing the properties of the welded joint. In this study, robotic flux cored arc welding with varying heat inputs (between 0.56-2.52 kJ/mm) was performed to determine the effect of heat input on weld microstructure, hardness, tensile properties, and impact toughness in the structural steel joints. Results exhibited that decrease in heat input from 2.52 to 0.56 kJ/mm changed the majority of the microstructure from polygonal ferrite to acicular ferrite. Furthermore, this increased by 56%, 37%, and 47% in yield strength, tensile strength, and hardness values, respectively, while decreasing by 30% and 15% in elongation and Charpy impact test results, respectively. Moreover, all welded joints displayed a satisfying toughness value higher than the requested value of 47 J, even at the test temperature of -50 °C. Finally, it can be concluded that the optimum results were obtained with a heat input of 1.26 kJ/mm, considering the minimum requirements of the AWS A5.20 standard and the expectations in applications.

Keywords: Robotic MAG welding, Flux-cored welding wire, Structural steel joints, Heat input, Microstructural characterization, Mechanical properties

FCAW Prosesi ile Yapısal Çeliklerin Birleştirilmesinde Isı Girdisinin Mikro yapı ve Mekanik Özelliklere Etkisi

Öz: Özlü kaynak telleri, yapısal ve boru hattı kaynağı, gemi yapımı, açık deniz inşaatları, petrokimya ve enerji üretim endüstrilerinde oldukça yaygın bir şekilde kullanılmaktadır. Çok pasolu kaynaklarda yüksek ısı girdileri, daha kısa üretim sürelerine neden olurken, kaynaklı birleştirmenin özelliklerini de önemli ölçüde değiştirmektedir. Bu çalışmada, yapısal çeliklerin kaynaklı birleştirmelerde ısı girdisinin kaynak mikroyapısı, sertlik, çekme özellikleri ve darbe tokluğu üzerindeki etkisini belirlemek için değişen ısı girdileriyle (0,56-2,52 kJ/mm arasında) robotik özlü özlü ark kaynağı yapılmıştır. Sonuçlar, ısı girdisinin 2.52'den 0.56 kJ/mm'e düşmesi ile mikro yapının genelinin poligonal ferritten asiküler ferrite dönüştüğünü göstermiştir. Bu da akma mukavemeti, çekme mukavemeti ve sertlik değerlerinde sırasıyla %56, %37 ve %47'lik bir artışa neden olurken, uzama ve Charpy darbe testi sonuçlarında sırasıyla %30 ve %15'lik bir düşüşe neden olmuştur. Ayrıca, kaynaklı birleştirmelerin tümünde -50 °C'lik test sıcaklığında bile istenen 47 J değerinden oldukça yüksek tokluk değerleri elde edilmiştir. Son olarak, AWS A5.20 standardının minimum gereksinimleri ve uygulamalardaki beklentiler dikkate alındığında optimum sonuçların 1,26 kJ/mm ısı girdisi ile elde edildiği sonucuna varılmıştır.

Anahtar Kelimeler: Robotik MAG kaynağı, Özlü kaynak teli, Yapısal çelik birleştirmeleri, Isı girdisi, Mikroyapı karakterizasyonu, Mekanik özellikler

* Department of Metallurgical and Materials Engineering, Engineering Faculty, İstanbul Gedik University, Cumhuriyet Mahallesi, İlkbahar Sokak, No: 1-3-5 Yakacık, 34876, Kartal, Istanbul, TÜRKİYE
Corresponding Author: Uğur GÜROL (ugur.gurol@yahoo.com)

1. INTRODUCTION

The flux cored arc welding (FCAW) wires are commonly used in structural and pipeline welding, shipbuilding, offshore constructions, petrochemical, and power generation industries where productivity, high deposition rates, and out-of-position welding are required (Pitrun et al., 2004), (Yang et al., 2020). FCAW wires are classified into three main types having different properties: rutile-based wires, metal-cored wires (MCW), and basic wires. MCW increases the deposition efficiency due to having no slag-forming elements in the filling (Gürol et al., 2022a). Basic wires produce a very fluid slag with a relatively low solidification temperature. The rutile-based wires lead to a more fluid slag which solidifies at a lower temperature and allows the weld bead to become flat with good wettability compared to others (Weman and Linden, 2006). FCAW wires are formulated to adapt to a specific shielding gas mixture by adding flux powders having different characteristics from the wire manufacturers. The shielding gases in FCAW defined in the EN 439 standard are argon, helium, carbon dioxide, oxygen, nitrogen, and hydrogen. The most used gas in the industry is 100% carbon dioxide because it is a relatively cheap shielding gas since it is readily available (Gürol et al., 2022b). It is also used as a component in argon-based mixtures (up to 25%) to combine the effects of both gases and achieve properties suitable for each situation.

Welding engineers are responsible for developing and working on the weld procedures in order to increase production efficiency. This is accomplished by higher heat inputs, higher travel speeds with the same heat input, and using multiple electrodes (Tandem). However, higher heat input results in significant changes in the microstructure of both the weld metal (WM) and the heat-affected zone (HAZ) (Viano et al., 2000), (Ling et al., 2015). Bang et al. (2014) studied the effect of welding parameters on the tensile properties of the WM obtained with AWS E80T1-Ni1 FCAW wire. They indicated tensile strength of the WM first increased (up to 2.1 kJ/mm), then decreased (between 2.1 and 4.5 kJ/mm) due to the microstructural change with the increase in heat input. Evans (1982) reported that increasing the heat input from 0.6 to 4.3 kJ/mm in all weld metals obtained by C–Mn iron powder basic electrodes reduced the tensile properties, and optimum Charpy results were obtained at about two kJ/mm. Muda et al. (2015) investigated the effect of three heat input combinations (0.99, 1.22, and 2.25 kJ/mm) on the ABS Grade A steel joints welded by the FCAW process. They reported that higher heat input caused grain coarsening, lower hardness, and lower impact toughness values than lower and medium heat input. Zhang et al. (2016) studied the effect of heat input and metal transfer on the weld geometry and microstructure of welding joints performed underwater using the wet FCAW method. They reported that the underwater welds have less acicular ferrite in the weld metal and less pro-eutectoid ferrite in the HAZ due to the rapid cooling effect and lower temperature compared with the air welds.

To summarize, the effect of the heat input on the properties of the weld joints can differ depending on the filler metal and base material used. Therefore, optimization studies for each welding combination are of great importance. In this study, the FCAW wire with the E71T-1C class wire described in AWS A5.20, having a commercial name of GeKa ELCOR R71, was used as filler metal. Robotic flux-cored arc welding with varying heat inputs (between 0.56-2.52 kJ/mm) was performed to determine the effect of heat input on weld microstructure, Vickers hardness, tensile properties, and impact toughness of structural steel joints.

2. MATERIALS AND METHODS

The robotic FCAW in a flat position was performed using E71T-1C class wire described in AWS A5.20 with a diameter of 1.2 mm as a filler metal. The S355-J2 structural steel plates with dimensions of 150x350x20 mm were used as base metal. The chemical composition of the welding wire and base metal given in the material certificates are shown in Table 1. The FCAW

wires used in the study are classified as exhibiting low spatter loss, a fast-freezing slag rutile-based slag, which completely covers the weld bead, and a spray arc transfer resulting in high deposition rates. The diffusible hydrogen content of the FCAW wire was determined by gas chromatography according to the EN ISO 3690 standard using the Bruker G4 Phoenix model of the diffused hydrogen meter. The average hydrogen content was found as 3.68 ml/100g. Welded joints having a configuration with a 60-degree single V groove edge and a root-face gap of 13 mm, as described in AWS A5.20, were obtained under 100 % CO_2 of shielding atmosphere with a flow rate of 15 l min^{-1} (Figure 1). The base plates were fixed during the experiments using a fixture to reduce welding-induced distortion.

Table 1. Chemical analysis of the welding wire and base metal (wt. %)

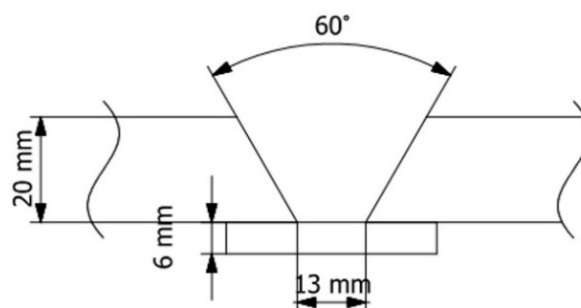|	C	Si	Mn	P	S
Base metal	0.13	0.22	1.45	0.015	0.005
E71T-1C wire	0.06	0.50	1.30	0.011	0.008

Figure 1:
The joint configuration

The heat input can be arranged by changing operational parameters such as welding current, voltage, and travel speed. However, by changing more than one parameter simultaneously, multiple factors could influence the results and make a distinct correlation between heat input and mechanical properties difficult (Schönmaier et al., 2021). Therefore, the four different heat inputs were arranged by changing only the travel speed, and the other parameters were kept constant. According to AWS A5.20, heat input values for the all-weld joints should meet the requirements of 1.0–2.0 kJ/mm for the filler materials having a diameter of 1.00-1.20 mm. In this study, the heat inputs were chosen as 2 of them remained within the range specified by the standard (1.26 and 1.01 kJ/mm), while the others (2.52 and 0.56 kJ/mm) were outside the value specified by the standard. The nominal heat inputs were calculated by equation 1, where Q is the heat input, in kJ/mm; V the arc voltage, in V; I the arc current, in A; S the velocity of the welding torch (mm/min), as stated in AWS A5.20 standard. Moreover, the inter-pass temperature was maintained at 150 ± 15 °C, and preheating was not applied. The welding parameters used in this study are presented in Table 2.

$$Q = (V \times I \times 60)/(1000 \times S) \qquad (1)$$

Table 2. Welding parameters, including heat input variation

Beads per layer	Number of layers	Current (A)	Voltage (V)	Welding speed (cm/min)	Nominal heat input per pass (kJ/mm)
1	10			20	2.52
2	8	250 - 260	32.8 – 33.2	40	1.26
3	7			50	1.01
4	9			90	0.56

An X-ray radiographic test (RT) was first conducted to detect any defects which may be present in all-weld joints using a portable industrial X-Ray generator that has a capacity of 300 kV. Upon completion of the X-ray testing, the welded joints were cut and machined to the required dimensions for preparing the metallographic and mechanical test specimens corresponding to AWS A5.20. Tensile and Charpy-V notch (CVN) test specimens were extracted in the mid-thickness section at the position corresponding to the WM central line, as shown in Figure 2. The notches of the CVN specimens were positioned through the thickness of the weld beads, and tests were conducted at varying temperatures at temperatures of -20, -30, -40, and -50 °C to detail the critical ductile-brittle transition zone. Tensile specimens were removed parallel to the welding direction, and tests were carried out with round bar specimens at ambient temperature. The Vickers-hardness tests (5 kg load) were performed on samples obtained through the thickness direction corresponding to the CVN test locations, marked in red dots shown in Figure 2.
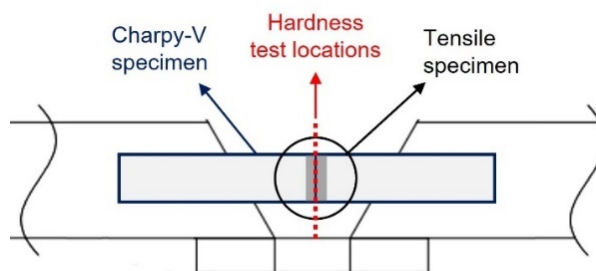

Figure 2:
Locations of test specimens

Standard metallographic procedures (such as grinding, polishing, and etching) for the cross-sectional specimens were performed to reveal the microstructural changes in relation to heat input variation utilizing an optical and scanning electron microscope. The macrostructural investigation was performed according to ISO 5817-B to detect any weld defects such as cracks, insufficient melting between the layers, etc. The fracture surface of CVN test specimens was also evaluated using a stereo microscope. Finally, the chemical analysis of the all-weld joints was carried out on the reduced section of tensile specimens using ARL OES 8860 optical emission spectrometer.

3. RESULTS AND DISCUSSION

Table 3 shows the chemical analysis of the joints obtained, including the Ceq value that indicates the hardenability of the joints. The C and Mn contents which are the primary elements that affect the Ceq, changed with heat input; however, the Mn amount seems more affected by heat input. The highest Ceq was obtained with the lowest heat input of 0.56 kJ/mm. However, the Ceq values decreased with an increase in heat input, indicating that sudden loss of Mn in the

WM. This was caused by the lowest boiling temperature and heat of vaporization of manganese compared to others existing in welding wire (Chinakhov et., 2016). A significant increase in C and Mn is visible with the decrease of the heat input from 1.01 to 0.56 kJ/mm.

Table 3. Chemical analysis of welded joints fabricated with varying heat inputs (wt. %)

Heat input (kJ/mm)	C	Si	Mn	P	S	(Cr+Mo+V +Ni+Cu)	Ceq
2.52	0.065	0.38	1.17	0.010	0.008	max. 0.2	0.28
1.26	0.063	0.41	1.21	0.008	0.008		0.28
1.01	0.069	0.39	1.25	0.012	0.008		0.30
0.56	0.082	0.44	1.41	0.015	0.008		0.34

The macrographs of the welded joints produced with varying heat inputs are shown in Figure 3. No welding defects that exceed the ISO 5817-B class were found in the macro section of the joints, such as porosity, crack, or others. It was also observed that all layers except for the final layers of the multi-pass joints were reheated by successive passes. Due to different heat inputs, all joints revealed completely different amounts of as-deposited (columnar) and reheated regions at the middle section of the joint that corresponds to the CVN test location. In addition, the heat-affected zone of base materials tends to get wider with increased heat input.
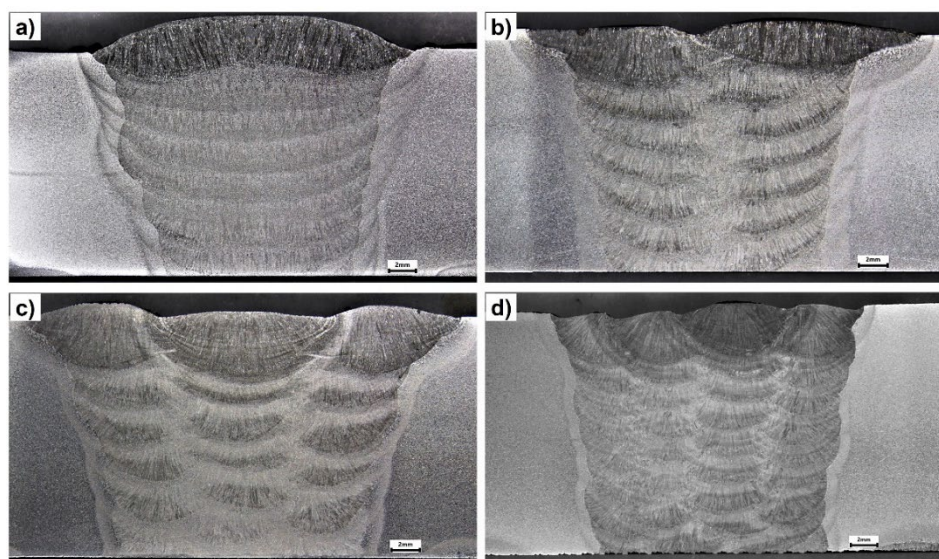

Figure 3:
Section view of the welded joints fabricated with a varying heat input of;
a.*2.52 kJ/mm **b.***1.26 kJ/mm **c.** *1.01 kJ/mm **d.** 0.56 kJ/mm*

The microstructure of face regions generally consists of a columnar structure (Figure 4). Their microstructure is composed mainly of acicular ferrite (AF) with different amounts of grain boundary ferrite (GBF) and ferrite side plates (FSP). However, the amount and width of FSP and GBF decreased clearly, and the microstructure became dominated by an acicular ferrite structure with decreasing heat input. As shown in Fig. 4d, in the case of welding with low heat input (0.56 kJ/mm), GBF and FSP almost disappeared, and the final microstructure was entirely composed of fine acicular ferrite structures. Similar microstructures were also reported to be formed in shielded metal arc welded, submerged arc welded, friction stir welded, or wire arc additive manufactured structural steels (Gürol et al., 2022a), (Jorge et al., 2019), (Evans, 1991), (Küçükömeroğlu et al., 2018), (İpekoğlu et al., 2018).
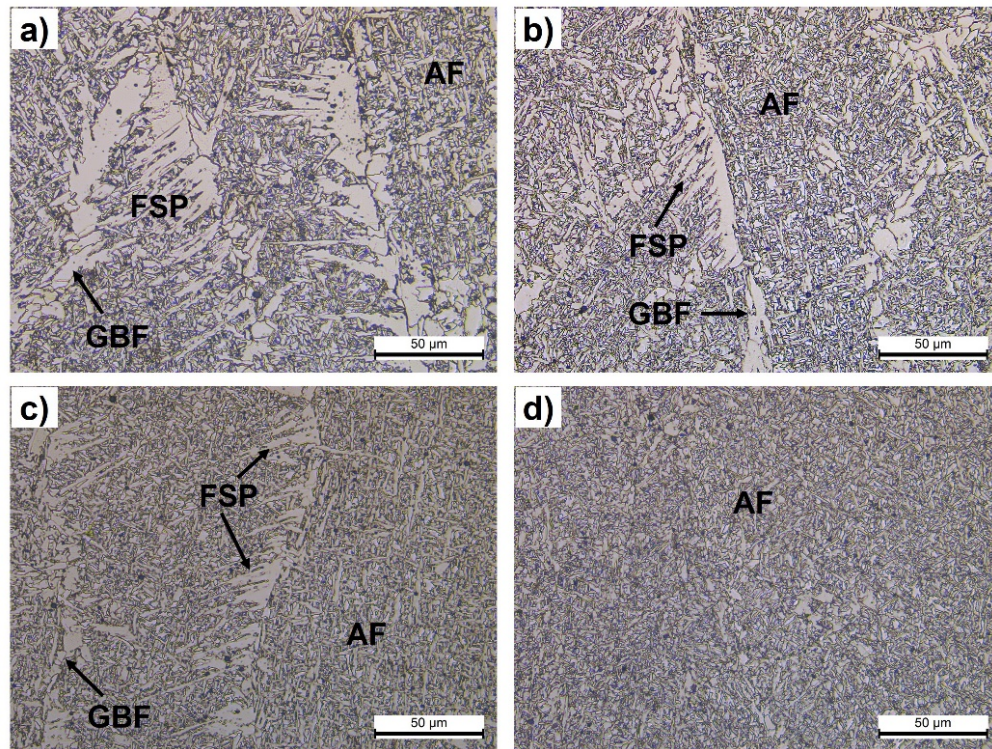
Figure 4:
Micrographs showing the microstructure of the face region with a varying heat input of;
a.*2.52 kJ/mm* **b.***1.26 kJ/mm* **c.** *1.01 kJ/mm* **d.** *0.56 kJ/mm*

The microstructure of the middle regions that correspond to the CVN test location observed by OM and SEM are shown in Figure 5 and Figure 6, respectively. It is well known that the impact toughness of multi-run weld metal depends on the amount of the as-weld and reheated regions (Wang et al., 2018). Especially, the majority of middle sections (CVN test locations) of the joints welded with higher heat inputs of 2.52 and 1.26 kJ/mm contained reheated regions, and their microstructure predominantly exhibited polygonal ferrite structures with a small amount of pearlite inside the austenite grain boundaries. Furthermore, the cooling rate after welding influences the transformation behavior and is commonly described as the cooling time from 800 °C to 500 °C ($\Delta t8/5$) (Zhou et al., 2018). In this context, the $\Delta t8/5$ cooling time of the joints welded with a heat input of 2.52, 1.26, 1.01, and 0.56 kJ/mm was calculated as 21.9 s, 7.6 s, 6.1 s, and 3.4 s according to EN 1011-2, respectively. Therefore, with the decrease of heat input from 2.52 to 1.26 kJ/mm, PF grains became smaller due to a shorter cooling time (Figure 6).

The majority of microstructure at the CVN test locations changed from polygonal ferrite to acicular ferrite in the joints welded with lower heat inputs of 1.01 and 0.56 kJ/mm. The main difference between the joints welded with 1.01 and 0.56 kJ/mm was found to be the amount of FSP and GBF phases at the columnar regions. As mentioned for the face regions, the amount of FSP and GBF were also reduced sharply, and AF grains became more smaller with the decrease of heat input from 1.01 to 0.56 kJ/mm at the CVN test locations. Moreover, randomly dispersed inclusions were found in all welds. The inclusions size exceeded 1.5 μm in high heat inputs, as shown in Figure 6. However, it became smaller than 1 μm with decreasing heat input to 0.56 kJ/mm, confirming increased nucleation sites for acicular ferrite. This also ensured that the inclusion's diameter depended on the heat input, as reported in a previous study (Viano et al., 2000).
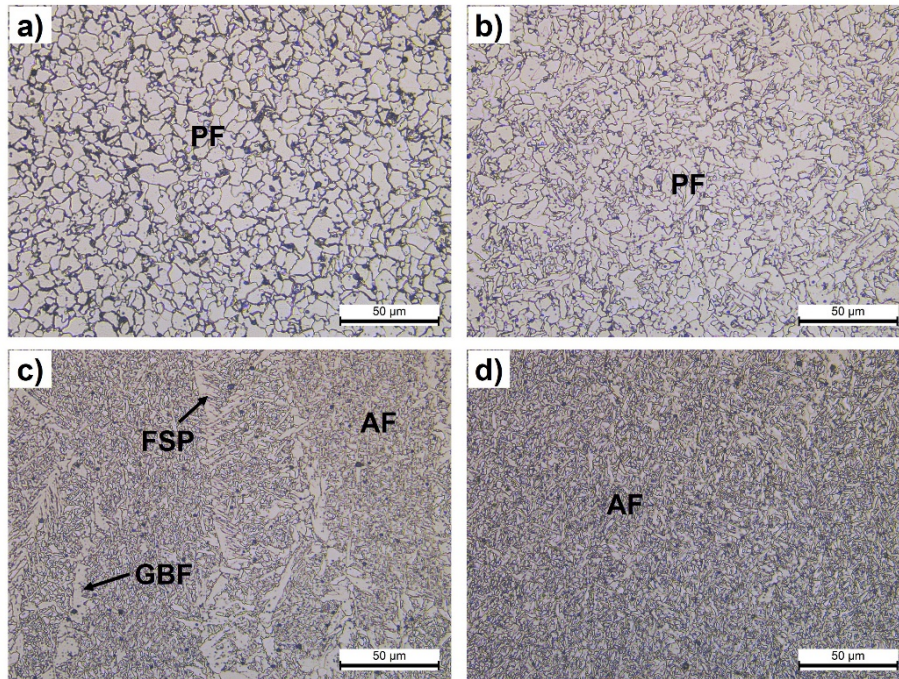
Figure 5:
Micrographs showing the microstructure of Charpy region with a varying heat input of;
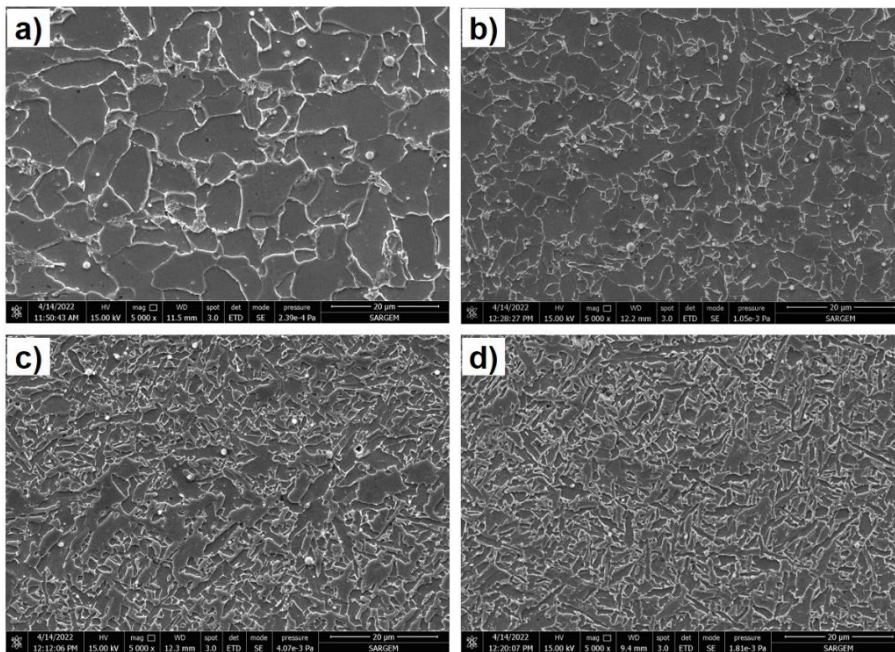***a.****2.52 kJ/mm* ***b.****1.26 kJ/mm* ***c.*** *1.01 kJ/mm* ***d.*** *0.56 kJ/mm*

Figure 6:
SEM micrographs showing the microstructure of Charpy region with a varying heat input of;
a.*2.52 kJ/mm* ***b.****1.26 kJ/mm* ***c.*** *1.01 kJ/mm* ***d.*** *0.56 kJ/mm*

Figure 7 shows the hardness test locations and test results of all the welded joints, containing both the as-deposited and reheated microstructures. All welded joints showed the same tendency that hardness results decrease first up to 3-4 mm below the surface due to the final layers having higher proportions of fine acicular ferrite structure resulting from faster cooling. The hardness values of the middle region corresponding to the CVN test locations were measured as 167±5 HV, 200±11 HV, 209±11 HV, and 246±11 HV for the heat inputs of 2.52, 1.26, 1.01, and 0.56 kJ/mm, respectively. The results reveal that heat input has a powerful effect on increasing the hardness of the WM by decreasing heat input. An example, a reduction in heat input from 2.52 to 0.56 kJ/mm resulted in a sharp increase in the hardness by about 48% at the CVN test location. Moreover, the scatter in hardness values of the CVN test location tended to increase with decreasing heat input, due to the formation of complex ferrite structures, especially in 1.01 kJ/mm heat input.
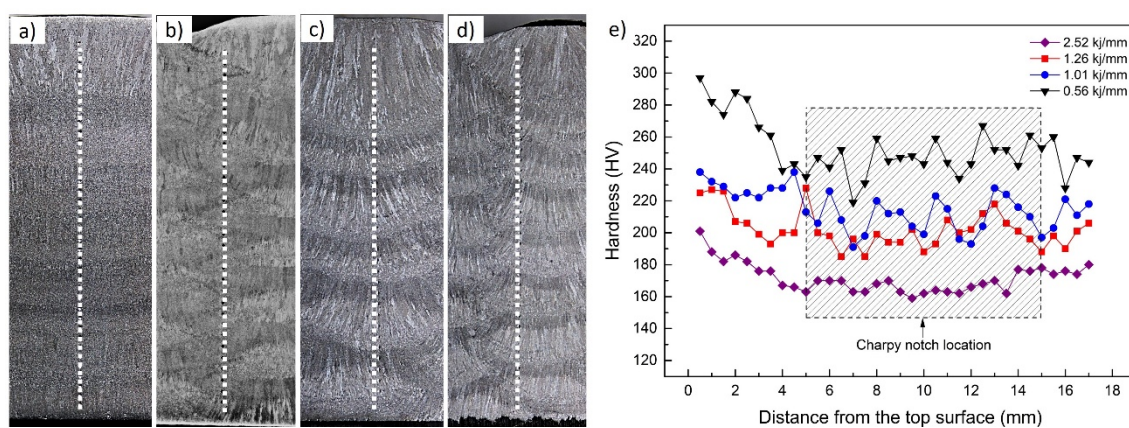

Figure 7:

Hardness test locations (marked with white dots) of the weld joints with a varying heat input of; a.2.52 kJ/mm b.1.26 kJ/mm c. 1.01 kJ/mm d. 0.56 kJ/mm e. hardness test results

The tensile test results with the minimum requirements of the AWS A5.20 standard were listed in Table 4, and results obtained from all the welded joints were compared in Figure 8. The tensile properties are more affected by the microstructure of all the welded joints composed of polygonal ferrite for both 2.52 and 1.26 kJ/mm and acicular ferrite for both 1.01 and 0.56 kJ/mm, which is predominant at the test location. As a result, the highest yield and tensile properties (694 MPa and 719 MPa, respectively) were achieved with the heat input of 0.56 kJ/mm. In contrast, the lowest (444 MPa and 524 MPa, respectively) were achieved with 2.52 kJ/mm. These results showed that the increased amount of acicular ferrite could result in a 56% (from 444 to 694 MPa) and 37% (from 524 to 719 MPa) increase in yield and tensile strength, respectively. However, the increase in yield strength led to a sharp decrease in elongation. Therefore, the minimum elongation value specified as 22% in AWS A5.20 was only obtained with heat inputs of 1.26 and 2.52 kJ/mm.

Table 4. Tensile test results of the welded joints fabricated using varying heat inputs

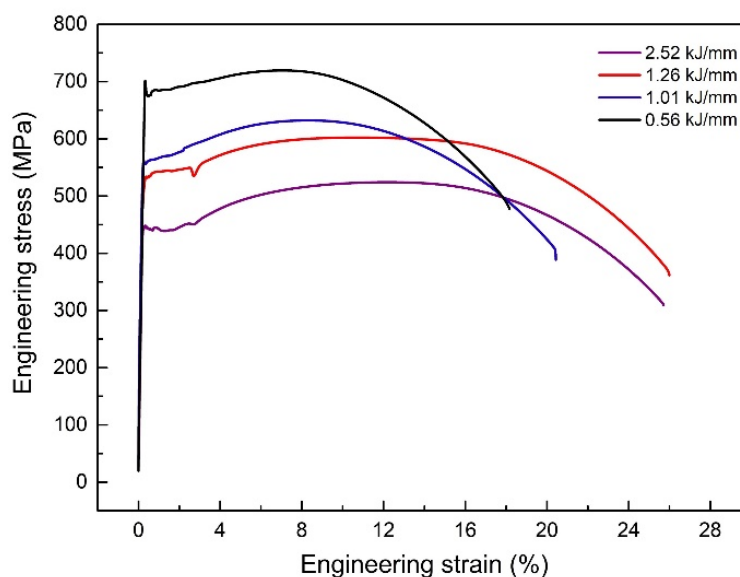|	Heat input (kJ/mm)	Yield strength (MPa)	Tensile strength (MPa)	Elongation (%)
AWS A5.20	1.00 – 2.00	Min. 390	490-670	Min. 22
ELCOR R71	2.52	444	524	25.6
	1.26	514	602	26.0
	1.01	561	632	20.4
	0.56	694	719	18.1

Figure 8:
Engineering stress–strain curve of the welded joints

The CVN test results are shown in Table 5. A considerable influence of test temperature on the impact toughness of the all-weld joints can be observed in Figure 9. Varying impact toughness values at different heat inputs were obtained due to the formation of different microstructural phases in the Charpy region. The general trend showed as decreasing the heat input resulted in a decrease in impact toughness values at all test temperatures except the heat input of 0.56 kJ/mm. The decrease in the amount of FSP and increase in AF amount at a heat input value of 0.56 kJ/mm caused higher Charpy results than the joint welded with a heat input of 1.01 kJ/mm. Nevertheless, the 47 J value specified in the related standards was obtained for all the joints even at -50° C, which is relatively high for rutile-based FCAW wire.

Table 5. Charpy impact test results of all the welded joints

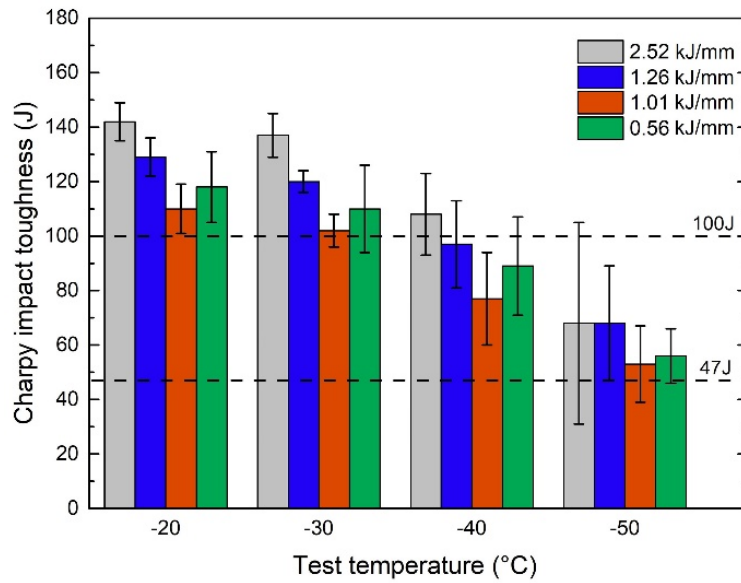| Heat input (kJ/mm)	Test temperature			
	-20 ºC	-30 ºC	-40 ºC	-50 ºC
2.52	142 ± 7	136 ± 7	108 ± 15	68 ± 37
1.26	129 ± 7	120 ± 4	97 ± 16	67 ± 21
1.01	110 ± 9	102 ± 6	77 ± 17	53 ± 13
0.56	118 ± 13	110 ± 17	89 ± 18	56 ± 10

Figure 9:
Comparison of the Charpy impact test results

Figure 10a-d shows the fracture surfaces of CVN test specimens taken from the joint welded with the highest heat input depending on the test temperature. All the specimens exhibited a mixture of shear and flat fracture regions. The shear regions are considered fully ductile, while the flat regions could be ductile, brittle, or a combination of both. In this context, the increased number of flat regions (shown in yellow) with a decrease in test temperature resulted in a decrease in toughness values.
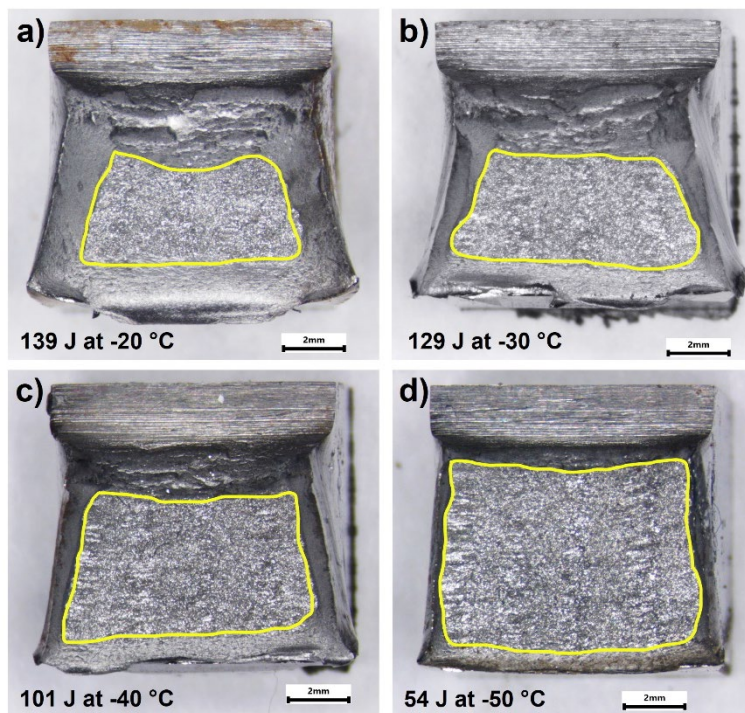

Figure 10:
Fracture view of the Charpy impact test specimens of the welded joint fabricated by using a heat input of 2.52 kJ/mm showing the total area of flat regions in yellow

4. CONCLUSIONS

In this study, the effect of different heat inputs on the microstructure and mechanical properties of structural steel joints obtained by the FCAW method using low alloyed steel wire described as E71T-1C in AWS A5.20 (ELCOR R71) was investigated, and the results were compared with each other. The obtained results can be summarized below.

- The increase in heat input caused a decrease in the amount of Mn in the all-weld metal deposit, due to Mn evaporation, resulting in a decrease in Ceq values which is also a reason for the change of microstructure and decrease in tensile strength of weld metal.
- The majority of microstructures at CVN test locations of the joints welded with higher heat inputs (2.52 and 1.26 kJ/mm) exhibited PF structures due to the higher amount of reheated regions existed while the majority of microstructures with lower heat inputs (1.01 and 0.56 kJ/mm) showed higher amount of AF with a small amount of GBF and FSP.
- The change of microstructure from polygonal ferrite to acicular ferrite due to the decreased heat input from 2.52 and 0.56 kJ/mm resulted in an increase of 56%, 37%, and 47% in the yield strength, tensile strength, and hardness values while resulting in a decrease of 30% and 15% in elongation and Charpy impact test results, respectively. However, all four joints displayed a satisfying toughness value higher than the requested value of 47 J even at the test temperature of -50 °C.

As a result of the study, it can be concluded that optimum test results were obtained with a heat input of 1.26 kJ/mm, considering the minimum requirements of the AWS A5.20 standard and the expectations in applications.

CONFLICT OF INTEREST

The author confirms that there is no known conflict of interest or common interest with any institution/organization or person.

AUTHOR CONTRIBUTION

Uğur Gürol takes all responsibility for the manuscript.

ACKNOWLEDGMENT

REFERENCES

1. Bang, K., Park, C., Jeong, H. (2014) Low heat input welding to improve impact toughness of multipass FCAW-S weld metal, *Journal of Ocean Engineering and Technology*, 28(6), 540-545. Doi: 10.5574/KSOE.2014.28.6.540

2. Chinakhov, D. A., Chinakhova, E. D., Sapozhkov, A. S. (2016) Manganese content control in weld metal during MAG welding, *IOP Conf. Series: Materials Science and Engineering*, 142, 012026. Doi: 10.1088/1757-899X/142/1/012026

3. Evans, G. M. (1982) The effect of heat-input on the microstructure and properties of C-Mn all-weld-metal deposits, *Welding Journal*, 61(04), 125-132, 1982.

4. Evans, G. M. (1991) The Effect of aluminium in shielded metal arc C-Mn steel multipass deposits, *Welding Research Supplement,* 32–40, 1991.

5. Gürol, U., Dilibal, S., Turgut, B., Koçak, M. (2022a) Characterization of a low-alloy steel component produced with wire arc additive manufacturing process using metal-cored wire, *Materials Testing*, 64(6), 755–767. Doi: 10.1515/mt-2021-2155

6. Gürol, U., Çoban, O., Coşar, İ., Koçak, M. (2022b) Effect of the notch location on the Charpy-V toughness results for robotic flux-cored arc welded multipass joints*, Materials Testing*, Doi: 10.1515/mt-2022-0113

7. İpekoğlu, G., Küçükömeroğlu, T., Aktarer S. M., Sekban, D. M., Çam, G. (2018) Microstructural characterization and mechanical properties of St37/St52 plates joined by friction stir welding, *Journal of Science and Engineering,* 20(59), 471-480, Doi: 10.21205/deufmd. 2018205937

8. Jorge J. C. F., Souza L. F. G., Araújo L. S., Bott I. S., Mendes, M. C., Evans, G. M. (2019) Microstructure and toughness of C-Mn steel submerged-arc weld deposits, with and without titanium addition, *IIW Annual Assembly*, Bratislava, Chech Republica, IIW Doc. IX-2674-19.

9. Küçükömeroğlu, T., Aktarer, S. M., İpekoğlu, G, Çam, G. (2018) Mechanical properties of friction stir welded St 37 and St 44 steel joints, *Materials Testing,* 60 (12), 1163-1170. Doi: 10.3139/120.111266

10. Ling, K. H., Fuh, Y. K., Kuo, T. C., Xun-Tu, S. (2015) Effect of welding sequence of a multi-pass temper bead in gas-shielded flux-cored arc welding process: hardness, microstructure, and impact toughness analysis, *International Journal of Advanced Manufacturing Technology,* 81, 1033–1046. Doi: 10.1007/s00170-015-7277-x

11. Muda, W. S. H., Nasir, N. S. M, Mamat, S., Jamian, S. (2015) Effect of welding heat input on microstructure and mechanical properties at coarse grain heat affected zone of ABS grade a steel, *ARPN Journal of Engineering and Applied Sciences*, 10(20), 9487-9495

12. Pitrun, M., Nolan, D., Dunne, D. (2004) Diffusible hydrogen content in rutile flux-cored arc welds as a function of the welding parameters, *Welding in the World*, 48, 2–13. Doi:10.1007/BF03266408

13. Schönmaier, H., Krein, R., Schmitz-Niederau, M., Schnitzer R. (2021) Influence of the heat input on the dendritic solidification structure and the mechanical properties of 2.25Cr-1Mo-0.25V submerged-arc weld metal. *Journal of Materials Engineering and Performance,* 30, 7138–7151. Doi: 10.1007/s11665-021-05922-x

14. Viano, D. M., Ahmet, N. U., Schumann, G. O. (2000) Influence of heat input and travel speed on microstructure and mechanical properties of double tandem submerged arc high strength low alloy steel weldments, *Science and Technology of Welding and Joining,* 5(1), 26-34. Doi: 10.1179/stw.2000.5.1.26

15. Wang, H. H., Tong, Z., Evans, G. M. (2018) Systematic role of Mn and Ti in microstructure and impact toughness of reheated C-Mn weld metals, *Proc. of the Intermediate Meeting of the IIW Sub. Commission 2C,* Genoa, IIW Doc. II-549-18.

16. Weman, K. and Linden, G. (2006) *MIG Welding Guide*, Woodhead Publishing Limited, Cambridge

17. Yang, L., Wang, Y., Sun, T., Huang, Y., Zhai, Y., He, T. (2020) Microstructure and mechanical properties of FCTIG-welded DH36 steel with rutile-type and basic-type flux

cored wires, *Journal of Materials Processing Technology*, 275, 116363. Doi: 10.1016/j.jmatprotec.2019.116363

18. Zhang, Y., Jia, C., Zhao, B., Hu, J., Wu, C. (2016) Heat input and metal transfer influences on the weld geometry and microstructure during underwater wet FCAW, *Journal of Materials Processing Technology*, 238, 373-382, Doi: 10.1016/j.jmatprotec.2016.07.024

19. Zhou, P., Wang, B., Wang, L., Hu, Y., Zhou, L. (2018) Effect of welding heat input on grain boundary evolution and toughness properties in CGHAZ of X90 pipeline steel, *Materials Science and Engineering: A,* 722, 112-121. Doi: 10.1016/j.msea.2018.03.029